

Tu P06 01

## A Single Euler Solution Per Anomaly

F.F. Melo (Observatorio Nacional), V.C.F. Barbosa\* (Observatorio Nacional), L. Uieda (Observatorio Nacional), V.C. Oliveira Jr (Observatorio Nacional) & J.B.C. Silva (Universidade Federal do Para)

### SUMMARY

---

We developed a method that drastically reduces the number of the source location estimates in Euler deconvolution to only one per anomaly. We use the analytical estimators of the Euler solutions. Our approach consists in detecting automatically the regions of the anomaly producing consistent estimates of the source horizontal coordinates. These regions form plateaus in the horizontal coordinate estimates using any structural index (defining the geometry of the sources). We identify these plateaus by fitting a first-degree polynomial to the horizontal coordinate estimates with a moving-window operator which spans these estimates. The places where the angular-coefficients estimates are closest to zero identify the plateaus of the horizontal coordinate estimates where consistent estimates of the horizontal source positions are found. The sample means of these horizontal coordinate estimates are the best estimates. The best structural index is the one that yields the minimum correlation between the total-field anomaly and the estimated base level over each plateau. By using the estimated structural index for each plateau, we extract the depth estimates over the corresponding plateau. The sample means of these estimates are the best depth estimates. Test on real data over alkaline bodies, central Brazil, retrieved sphere-like sources suggesting 3D bodies.

## Introduction

By using the theoretical basis proposed by Silva and Barbosa (2003), we present a new method for selecting the best 3D Euler solutions. Our method takes advantage of the contrasting behaviour of the 3D Euler solutions at the borders (forming inclined plans) and at the neighborhood of the highest absolute values of the anomaly (forming plateaus). Our method automatically delineates the plateaus, pointed out by Silva and Barbosa (2003), by fitting a first-degree polynomial to these estimates in a moving-window scheme spanning all estimates. The positions where the angular coefficient estimates are closest to zero identify the plateaus of the horizontal coordinate estimates. The sample means of these horizontal coordinate estimates are the best horizontal location estimates. These plateaus are horizontally well separated from each other and thus their horizontal positions can be easily recognized through a cluster analysis. Each subset of horizontal coordinates defining a plateau (and consequently the horizontal position of an anomalous source) is used to pick out the best estimates of the horizontal coordinates in Euler deconvolution. Next, for each anomalous source, our approach calculates the means of the estimates of the horizontal source positions over the associated plateau. For each plateau, our method determines the structural index via Barbosa et al.'s (1999) method and picks out the estimates of the depths over the corresponding plateau. Finally, the mean of the estimates of the source depth are calculated for each anomalous source. For each magnetic anomaly, our method provides a single source position.

## Method

Let's assume a magnetic point (or line) source at the coordinates  $(x_o, y_o, z_o)$  referred to a right-hand Cartesian coordinate system with the  $z$ -axis pointing downward. The observed total-field anomaly  $h \equiv h(x,y,z)$  at the coordinates  $(x, y, z)$  produced by this simple magnetic source obeys Euler's 3D equation (Reid et al., 1990). By considering a discrete set of observations of total-field anomaly, the classical formulation of 3D Euler deconvolution can be written as a linear system of equations given by

$$x_o \frac{\partial h_i}{\partial x} + y_o \frac{\partial h_i}{\partial y} + z_o \frac{\partial h_i}{\partial z} + \eta b = x_i \frac{\partial h_i}{\partial x} + y_i \frac{\partial h_i}{\partial y} + z_i \frac{\partial h_i}{\partial z} + \eta h_i, \quad i = 1, \dots, N, \quad (1)$$

where  $h_i \equiv h(x_i, y_i, z_i)$  is the  $i$ th observation of the total-field anomaly at the coordinates  $(x_i, y_i, z_i)$ ,  $b$  is a base level (i.e., a constant background value) and  $\eta$  is the structural index related to the nature or geometry of the source. For a given structural index, the 3D Euler deconvolution consists in solving the system of equations (1), in the least-squares sense, for the unknown parameters  $x_o$ ,  $y_o$ ,  $z_o$ , and  $b$ . In interpreting noisy and interfering total-field anomalies from a complex geologic setting, the 3D Euler deconvolution uses a moving-data window scheme. By using the observations inside a data window, the Euler deconvolution obtains the estimates  $\hat{x}_o$ ,  $\hat{y}_o$ ,  $\hat{z}_o$ , and  $\hat{\mathcal{L}}$  for each position of a moving-data window. As pointed out by Barbosa and Silva (2011), this procedure has the disadvantage of estimating a large number of inconsistent solutions making it difficult to decide on the correct source position. Silva and Barbosa (2003) deduced the analytical estimators for parameters  $x_o$ ,  $y_o$  and  $z_o$  and proved their bias and symmetry properties as a function of the  $x$ - and  $y$ -coordinates of the center of the moving-data window. At the anomaly borders, the estimates  $\hat{x}_o$ ,  $\hat{y}_o$  and  $\hat{z}_o$  are biased toward the arithmetic averages of the respective  $x$ -,  $y$ - and  $z$ -coordinates of the center of the moving-data window. This happens regardless of the assumed  $\eta$  and regardless of the source magnetization vector. Conversely, in the neighborhood of the highest absolute values of the total-field anomaly the estimates  $\hat{x}_o$ ,  $\hat{y}_o$  and  $\hat{z}_o$  are nearly constant values defining a plateau. Specifically, at this plateau, the estimates  $\hat{x}_o$  and  $\hat{y}_o$  are very close to the respective  $x$ - and  $y$ -coordinates of the true source, independently of the assumed  $\eta$  and independently of the source magnetization vector. However, the estimates  $\hat{z}_o$ , on this plateau, are very close to the depth of the true source only if the assumed  $\eta$  is correct; otherwise, the estimates  $\hat{z}_o$  will underestimate (or overestimate) the depth of the true source if the assumed  $\eta$  is smaller (or greater) than the correct one. We take advantage of this behaviour of the Euler solutions in producing plateaus to compute the best estimates of horizontal positions ( $\tilde{x}_o, \tilde{y}_o$ ) and the depth ( $\tilde{z}_o$ ) of the source.

**Selecting the best horizontal coordinate estimates in Euler deconvolution** - First, we apply the 3D Euler deconvolution with any structural index. For each position of the moving-data window, we produce the plots of  $\hat{x}_o$  and  $\hat{y}_o$  against the  $x$ - and  $y$ -coordinates of the center of the moving-data window. To identify the plateaus in the plots of  $\hat{x}_o$  and  $\hat{y}_o$ , we take advantage of the fact that, at the borders of the anomaly, the estimates of  $\hat{x}_o$  and  $\hat{y}_o$  are biased toward the arithmetic averages of the respective,  $x$ - and  $y$ -coordinates of the center of the moving-data window, forming inclined plans. Here, to differentiate the plateaus from inclined planes on the estimates  $\hat{x}_o$  and  $\hat{y}_o$ , first-degree polynomials are fitted, in the least-squares sense, to these estimates. This fitting will be accomplished through a moving-window scheme spanning the maps of the estimates of  $\hat{x}_o$  and  $\hat{y}_o$  on the plane of the  $x$ -coordinates against the  $y$ -coordinates of the center of the moving window. Next, the estimated angular coefficients of the fitted polynomials are plotted against the center of the moving window. Then, the places where the corresponding angular coefficients estimates are closest to zero identify the plateaus related to  $\hat{x}_o$  and  $\hat{y}_o$ . Then we compute the means ( $\tilde{x}_o$  and  $\tilde{y}_o$ ) of the estimates of the horizontal source positions ( $\hat{x}_o$  and  $\hat{y}_o$ ) over each plateau.

**Selecting the structural index ( $\eta$ )** - Based on Euler's equation, Barbosa et al. (1999) show that the estimates of the base level ( $\hat{b}$ ), as a function of the center of the moving-data window, are correlated with the observed total-field anomaly ( $h$ ). A minimum correlation between the estimates  $\hat{b}$  and  $h$  is favored when the correct  $\eta$  is assumed. To determine the correct  $\eta$  we first obtain estimates  $\hat{b}$  by using the classical Euler deconvolution for a number of tentative structural indices. Next, we select the subsets of the total-field anomaly and estimates  $\hat{b}$  that approximately fall within the plateaus identified in the plots of  $\hat{x}_o$  and  $\hat{y}_o$ . Finally, for each tentative  $\eta$ , we compute the correlation coefficient between these subsets of the total-field anomaly and of the estimates  $\hat{b}$ . The tentative  $\eta$  that produces the minimum correlation coefficient (in modulus) is the best estimate of the structural index.

**Selecting the best depth estimates in Euler deconvolution** - At the plateaus in the plots of  $\hat{z}_o$ , the estimates  $\hat{z}_o$  are very close to the depth of the true source only if the assumed structural index is correct (Silva and Barbosa, 2003). Using the best estimate of the structural index ( $\eta$ ), our practical procedure begins by producing a plot of all these estimates  $\hat{z}_o$  against the  $x$ - and  $y$ -coordinates of the center of the moving-data window. Next, we determine the intersection of the sets of estimates  $\hat{x}_o$  and  $\hat{y}_o$  defining plateaus and extract the subset of the estimates  $\hat{z}_o$  that fall within this intersection. Finally, we compute the sample mean  $\tilde{z}_o$  of the extracted subset of the estimates  $\hat{z}_o$ . This sample mean  $\tilde{z}_o$  is taken as the best depth estimate of the source.

**Geologic setting with multiple sources** - In real word scenarios where the observed total-field anomaly is produced by several sources, we need to identify and individualize each of the plateaus occurring in the plots of  $\hat{x}_o$  and  $\hat{y}_o$  to select the best horizontal coordinate estimates of each source. To map automatically each plateau we proceed exactly as was done in the case of a single source. Then we discriminate among the subsets of the  $x$ - and  $y$ -coordinates related to each plateau using a cluster analysis algorithm. After discriminating each plateau in the plots of  $\hat{x}_o$  and  $\hat{y}_o$ , the above-explained approaches are applied to each plateau as in the case of a single source.

### Applications to synthetic data

We computed the noise-corrupted total-field anomaly produced by four spherical sources emplaced in a nonmagnetic medium. The radii of all spheres are 1 km and they are magnetized uniformly by induction only, having a magnetization with intensity of 4 A/m, inclination of 60° and declination of 20°. These spheres are at the same depth of 2 km. The true horizontal coordinates of the centers of the

four spheres are:  $x_o = 10, 18, 30,$  and  $35$  km; and  $y_o = 20, 12, 25$  and  $15$  km. The first step is to estimate the horizontal source positions. To do this, we apply the 3D Euler deconvolution using a moving-data window of  $15 \times 15$  grid points and assuming any structural index. Figures 1a and 1b show the estimates  $\hat{x}_o$  and  $\hat{y}_o$  against the  $x$ - and  $y$ -coordinates of the center of the moving-data window. We can see the overall trend of an inclined plane, and the presence of four local plateaus. The estimates  $\hat{x}_o$  and  $\hat{y}_o$  over these plateaus are very close to the respective true source positions  $x_o$  and  $y_o$ .

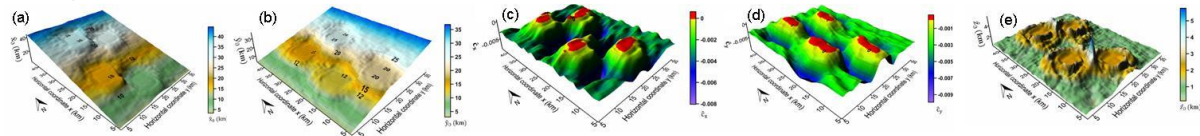


**Figure 1** Euler horizontal estimates  $\hat{x}_o$  (a) and  $\hat{y}_o$  (b). Angular coefficient estimates (c)  $\hat{c}_x$  and (d)  $\hat{c}_y$ . Euler depth estimates  $\hat{z}_o$  (e) against the  $x$ - and  $y$ -coordinates of the moving-window center with  $\eta=3$ .

The second step consists in identifying automatically the plateaus in the map of estimates  $\hat{x}_o$  and  $\hat{y}_o$ . We fit a first-degree polynomial to  $\hat{x}_o$  in a moving-window scheme and plot the estimated  $x$ -coefficients,  $\hat{c}_x$  against the  $x$ - and  $y$ -coordinates of the moving-window center. Analogously, this procedure is used to identify the plateaus in the map of estimates  $\hat{y}_o$ . The places where the estimated angular coefficients  $\hat{c}_x$  and  $\hat{c}_y$  are closest to zero (red areas in Figures 1c and 1d) identify the plateaus of  $\hat{x}_o$  and  $\hat{y}_o$ . In the third step, we automatically extract the subsets of the  $\hat{x}_o$  and  $\hat{y}_o$  estimates that fall within the respective plateaus. Then, we compute the sample means  $\tilde{x}_o$  and  $\tilde{y}_o$  of the respective subsets of the  $\hat{x}_o$  and  $\hat{y}_o$  estimates which will be taken as the best estimate of the source position along the  $x$ - and  $y$ -directions. Because there are four plateaus on the maps of  $\hat{x}_o$  and  $\hat{y}_o$ , there will be four sample means of the estimates  $\hat{x}_o$  and  $\hat{y}_o$  calculated over each plateau. These sample means are the best horizontal positions of the four bodies:  $\tilde{x}_o = 9.95, 17.94, 29.99$  and  $34.99$  km; and  $\tilde{y}_o = 20.00, 11.99, 25.04,$  and  $14.97$  km. The fourth step consists in determining the structural index of each source. For all sources, the best estimate of the structural index is 3 indicating that the sources are dipoles (spheres). In the fifth step we obtain the best depth estimates of each source. We apply the 3D Euler deconvolution assuming the best estimate for the structural index ( $\eta=3$ ). Because the best estimate of the structural index is the same for all sources, we produce only one map of the estimates  $\hat{z}_o$  (Figure 1e). To estimate the best  $\tilde{z}_o$  for each source, we pick out those estimates  $\hat{z}_o$  over the intersections (not shown) of the pairs of plateaus of  $\hat{x}_o$  and of  $\hat{y}_o$ . The sample means of the selected estimates  $\hat{z}_o$ , which in turn will be taken as the best depth estimates  $\tilde{z}_o$  of each source, are  $\tilde{z}_o = 2.07, 2.08, 2.10,$  and  $2.08$  km.

### Application to real data

Figure 2a shows the aeromagnetic total-field anomaly over mafic-ultramafic alkaline bodies, in central Brazil (Dutra and Marangoni, 2009). The flight height was 150 m above the ground surface. The strong magnetic anomalies have been named Morro do Engenho (ME) and A2 anomalies. The ME anomaly is produced by an alkaline outcropping body intruded in sediments. The A2 anomaly is a possible buried alkaline body being overlaid by the Quaternary sediments. We apply the 3D Euler deconvolution using a  $15 \times 15$  moving-data window spanning the study area. By assuming any structural index, we estimate  $\hat{x}_o$  (Figure 2b) and  $\hat{y}_o$  (Figure 2c) against the  $x$ - and  $y$ -coordinates of the center of the moving-data window. Two plateaus are easily detected by visual inspection of the estimated maps of  $\hat{x}_o$  and  $\hat{y}_o$ . We fit first-degree polynomials to the estimates  $\hat{x}_o$  and  $\hat{y}_o$ . Figures 2d

and 2e show the estimated angular coefficients  $\hat{c}_x$  and  $\hat{c}_y$ , where we can easily identify areas (in red) closest to zero. These red areas define the two subsets of the  $x$ - and  $y$ -coordinates which will be used to define the positions of the two plateaus on the maps of  $\hat{x}_o$  and  $\hat{y}_o$ . After locating these plateaus, we computed the two sample means  $\tilde{x}_o$  and  $\tilde{y}_o$  of the two subsets of the  $\hat{x}_o$  and  $\hat{y}_o$  estimates lying over each plateau. These sample means are the best horizontal positions of the ME body ( $\tilde{x}_o = 11.50$  km and  $\tilde{y}_o = 15.40$  km) and of the A2 body ( $\tilde{x}_o = 23.83$  km and  $\tilde{y}_o = 36.35$  km). We estimated the structural index of each body (Barbosa et al., 1999). Both bodies are interpreted as dipoles (spheres). Figure 2f shows the estimates  $\hat{z}_o$ . We computed the sample means  $\tilde{z}_o$  of the corresponding estimates  $\hat{z}_o$  located over the intersections of the pairs of plateaus of  $\hat{x}_o$  and of  $\hat{y}_o$ . Hence, we found that ME and A2 bodies are two sphere-like sources whose centers are located at depths of 3 and 3.2 km, respectively.

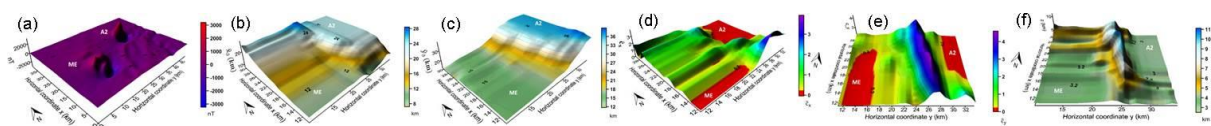


**Figure 2** Alkaline bodies, Brazil: (a) Total-field anomaly. Morro do Engenho (ME) and A2 anomalies. Euler horizontal estimates  $\hat{x}_o$  (b) and  $\hat{y}_o$  (c). Angular coefficient estimates (d)  $\hat{c}_x$  and (e)  $\hat{c}_y$ . Euler depth estimates  $\hat{z}_o$  (f) against the  $x$ - and  $y$ -coordinates of the moving-window with  $\eta=3$ .

## Conclusions

We have presented a new method for selecting the best source location estimates in 3D Euler deconvolution. Our approach has drastically reduced the number of the selected 3D Euler solutions to only one per anomaly. This is possible because our method does not select Euler solutions based on their statistical consistency after a cluster analysis. Rather, in our method this selection is grounded on the theoretical analysis of the estimators for the horizontal and vertical source positions in 3D Euler deconvolution as a function of the  $x$ - and  $y$ -coordinates of the observations. Our approach consists in detecting automatically the regions of the anomaly producing consistent estimates of the source horizontal coordinates.

## Acknowledgements

This research is supported by the Brazilian agencies CNPq, FAPERJ and CAPES.

## References

- Barbosa, V.C.F. and Silva, J.B.C. [2011] Reconstruction of geologic bodies in depth associated with a sedimentary basin using gravity and magnetic data. *Geophysical Prospecting*, **59**, 1021–1034.
- Barbosa, V.C.F., Silva, J.B.C. and Medeiros W.E. [1999] Stability analysis and improvement of structural index estimation in Euler deconvolution. *Geophysics*, **64**(1), 48–60.
- Dutra, A.C. and Marangoni, Y.R. [2009] Gravity and magnetic 3-D inversion of Morro do Engenho complex, central Brazil. *Journal of South American Earth Sciences*, **28**, 193–203.
- Reid, A.B., Allsop, J.M., Granser, H., Millet, A. J. and Somerton, I.W. [1990] Magnetic interpretation in three dimensions using Euler deconvolution. *Geophysics*, **55**(1), 80–91.
- Silva J.B.C. and Barbosa, V.C.F. [2003] 3D Euler deconvolution: Theoretical basis for automatically selecting good solutions. *Geophysics*, **68**(6), 1962–1968.